Biomaterials 318 (2025) 123148

Contents lists available at ScienceDirect

Biomaterials

journal homepage: www.elsevier.com/locate/biomaterials

# Two-dimensionally cultured functional hepatocytes generated from human induced pluripotent stem cell-derived hepatic organoids for pharmaceutical research

Jumpei Inui [a], Yukiko Ueyama-Toba [a,b,c,d], Chiharu Imamura [b], Wakana Nagai [b], Rei Asano [a], Hiroyuki Mizuguchi [a,b,c,d,e,f,*]

[a] Laboratory of Biochemistry and Molecular Biology, Graduate School of Pharmaceutical Sciences, Osaka University, Osaka, 565-0871, Japan
[b] Laboratory of Biochemistry and Molecular Biology, School of Pharmaceutical Sciences, Osaka University, Osaka, 565-0871, Japan
[c] Laboratory of Functional Organoid for Drug Discovery, National Institute of Biomedical Innovation, Health and Nutrition, Osaka, 567-0085, Japan
[d] Integrated Frontier Research for Medical Science Division, Institute for Open and Transdisciplinary Research Initiatives, Osaka University, Suita, Osaka, 565-0871, Japan
[e] Global Center for Medical Engineering and Informatics, Osaka University, Osaka, 565-0871, Japan
[f] Center for Infectious Disease Education and Research (CiDER), Osaka University, Osaka, 565-0871, Japan

ARTICLE INFO

*Keywords:*
Human induced pluripotent stem cells
Hepatic organoids
Drug-induced hepatotoxicity
Drug metabolism

ABSTRACT

Human induced pluripotent stem (iPS) cell-derived hepatocyte-like cells (HLCs) are expected to replace primary human hepatocytes (PHHs) as a new stable source of hepatocytes for pharmaceutical research. However, HLCs have lower hepatic functions than PHHs, require a long time for differentiation and cannot be prepared in large quantities because they do not proliferate after their terminal differentiation. To overcome these problems, we here established hepatic organoids (iHOs) from HLCs. We then showed that the iHOs could proliferate approximately $10^5$-fold by more than 3 passages and expressed most hepatic genes more highly than HLCs. In addition, to enable their widespread use for in vitro drug discovery research, we developed a two-dimensional culture protocol for iHOs. Two-dimensionally cultured iHOs (iHO-Heps) expressed most of the major hepatocyte marker genes at much higher levels than HLCs, iHOs, and even PHHs. The iHO-Heps exhibited glycogen storage capacity, the capacity to uptake and release indocyanine green (ICG), albumin and urea secretion, and the capacity for bile canaliculi formation. Importantly, the iHO-Heps had the activity of major drug-metabolizing enzymes and responded to hepatotoxic drugs, much like PHHs. Thus, iHO-Heps overcome the limitations of the current models and promise to provide robust and reproducible pharmaceutical assays.

## 1. Introduction

The liver plays a central role in the metabolism, uptake, and excretion of xenobiotics, including drugs, and it is frequently a target for drug toxicity. Therefore, evaluation using functional human hepatocytes is important for accurate prediction of the in vivo metabolism and toxicity of drugs. Primary human hepatocytes (PHHs) are the current gold standard in drug discovery research because they retain the activity of drug-metabolizing enzymes and transporters [2]. However, PHHs do not proliferate in vitro. Even long-term culture of PHHs has been considered difficult due to their rapid deterioration of hepatic functions, such as albumin excretion and drug-metabolizing activity, after seeding. Recently, several methods have been reported to overcome these drawbacks. In particular, PHHs cultured using either chemical reprogramming methods or organoid culture methods have been found to proliferate over the long term [3–8].

Human induced pluripotent stem (iPS) cell-derived hepatocyte-like cells (HLCs) are expected to replace PHHs as a new stable source of hepatocytes for pharmaceutical research [9,10]. Since human iPS cells can be generated from individuals with diverse genetic backgrounds, human iPS cell-derived HLCs can be used as an in vitro hepatocyte model reflecting the diversity in drug metabolism capacity by single

* Corresponding author. Laboratory of Biochemistry and Molecular Biology, Graduate School of Pharmaceutical Sciences, Osaka University, 1-6 Yamadaoka, Suita, Osaka, 565-0871, Japan.
*E-mail addresses:* inui-j@phs.osaka-u.ac.jp (J. Inui), toba-y@phs.osaka-u.ac.jp (Y. Ueyama-Toba), imamurachiharu838@gmail.com (C. Imamura), nagai-w@phs.osaka-u.ac.jp (W. Nagai), asano-r@phs.osaka-u.ac.jp (R. Asano), mizuguch@phs.osaka-u.ac.jp (H. Mizuguchi).

https://doi.org/10.1016/j.biomaterials.2025.123148
Received 27 September 2024; Received in revised form 24 January 2025; Accepted 26 January 2025
Available online 28 January 2025

nucleotide polymorphisms (SNPs) [11]. However, human iPS cell-derived HLCs also have lower hepatic functions, including drug-metabolizing enzyme activities, than PHHs [11–13]. In addition, HLCs require a long time for differentiation from human iPS cells and do not proliferate after their terminal differentiation, making the provision of a large supply of HLCs both expensive and labor-intensive. Moreover, high batch-to-batch variations of the hepatic functions in HLCs occur over the long differentiation period. These problems must be overcome before HLCs can be adopted for wide use.

Three-dimensional cell clusters called organoids can mimic the physiological and structural features of organs and tissues. Organoid technology enables functionally differentiated cells to maintain their functions and expand for a long-term period in vitro [14,15]. In the case of human iPS cell-derived hepatocyte organoids, the definition is ambiguous, ranging from cells that can actively proliferate to those that rarely proliferate but are structurally well developed [15–25]. Takebe et al. reported the generation of multicellular organoids called liver buds from human iPS cell-derived hepatic endoderm, endothelium, and septum mesenchyme [18,26]. Their organoids had vasculature and liver-like structures, making them suitable for liver transplantation and studies of liver development. On the other hand, their organoids did not proliferate and were difficult to culture for a long-term, and the activity levels of their drug-metabolizing enzymes were unknown. Their group also reported a high-throughput model of expandable hepatic organoids with a simpler structure [19,27]. Although these simpler organoids successfully reproduced bile transport, the details of their drug-metabolizing ability remained unclear, limiting their use in drug discovery research. Kim et al. reported expandable organoids from human iPS cell-derived hepatic endodermal cells and demonstrated that they metabolize drugs by cytochrome P450 (CYP) enzymes [20]. However, the drug-metabolizing capacity of these organoids did not reach that of PHHs, and their functional maturation took about 3 weeks. Therefore, it is currently difficult to achieve both cell proliferation and functional maturation in human iPS cell-derived hepatic organoids, and it still takes time and effort to switch the cells from a proliferative to a maturation state. Furthermore, unlike conventional two-dimensional (2D) cultured cells, organoids are embedded in Matrigel, which limits their general application.

In this study, we sucssesfully established human iPS cell-derived hepatic organoids (iHOs). We then optimized the maintenance medium for iHOs and identified the most suitable hepatocyte differentiation stage for the establishment of iHOs. Under optimal conditions, iHOs showed a high cell-proliferation capacity for more than 10 passages and higher expression of most hepatic genes than HLCs. Finally, we developed a 2D culture method in step-wise differentiation medium for 11 days. The 2D culture of iHOs not only matured them into hepatocytes with major hepatic functions, including high drug-metabolizing enzyme activities similar to those in PHHs, but also yielded iHOs with greater versatility for drug discover research compared to 3D-based organoid culture. The method shown in this study will thus provide powerful support for efficient drug discovery research using human hepatocytes.

## 2. Results

### 2.1. Suitable media for the establishment and culture of hepatic organoids

As a first step toward the establishment and culture of hepatic organoids, we examined suitable media. HLCs were prepared according to our previously reported method [28]. HLCs showed a hepatocyte-like polygonal cell morphology and expressed major hepatocyte marker proteins and genes (Fig. S1). The hepatic gene expression levels, CYP3A4 activity, and ALB/urea secretion levels in HLCs generated in this study were comparable to those in our recent previous reports [28–31]. For the establishment of organoids, HLCs were dissociated into single cells and suspended in Matrigel (Fig. 1A). We prepared two media, Hep-Medium and Chol-Medium, based on previous reports [7, 32], which were used for the establishment and culture of organoids from human and mouse hepatocytes. After one week, the organoids emerged from single HLC in both media. In Hep-Medium, iHOs had a spherical morphology with a thick cell layer and were composed of cells with a hepatocyte-like polygonal morphology (Fig. 1B). In contrast, the cell layer of iHOs cultured with Chol-Medium was thin and the cell morphology was unclear (Fig. 1C). The iHOs cultured with either medium were passaged at a ratio of 1:10 to 1:20 every week. The iHOs grew to about $10^5$-fold in 18 days with Hep-Medium, which was 100 times faster than the growth rate with Chol-Medium (Fig. 1D). The gene expression levels of hepatocyte markers (*albumin, ALB; hepatocyte nuclear factor 4 alpha, HNF4α; cytochrome P450 3A4, CYP3A4; cytochrome P450 2C9, CYP2C9; cytochrome P450 2C19, CYP2C19; uridine diphosphate glucuronosyltransferase 1A1, UGT1A1*) and cholangiocytes/progenitor markers (*epithelial cell adhesion molecule, EpCAM; Cytokeratin 7, CK7; Cytokeratin 19, CK19, luecine-rich orphan G-protein-coupled receptor, LGR5*) were analyzed by real-time RT-PCR. Hep-Medium increased the expression of most hepatocyte marker genes in iHOs more than twofold compared to the levels in HLCs and maintained this trend until at least the 10th passage. The gene expression of ALB was decreased by organoid culture with Hep-Medium (Fig. 1E). On the other hand, Chol-Medium was less effective at improving these gene expressions: the expression levels at the 10th passage were lower than those in HLCs (Fig. 1F). In addition, Chol-Medium increased the expression of cholangiocytes/progenitor marker genes in iHOs more than Hep-Medium (Fig. S2). These results suggested that Hep-Medium was more suitable for the establishment and culture of iHOs than Chol-Medium. We also examined differentiation medium (Diff-Medium), which was reported to be capable of maturation of human and mouse hepatocyte organoids [7]. However, the gene expression levels of hepatocyte markers in iHOs cultured with Diff-Medium were comparable to those in iHOs cultured with Hep-Medium (Fig. S3). Therefore, it was suggested that differentiation medium is not suitable for maturation of iHOs.

To investigate the optimal differentiation stage of HLCs for the establishment of organoids by Hep-Medium, we established organoids from cells at different hepatic differentiation stages (day9, day14, day25). Hepatocyte marker genes were stably expressed at higher levels in organoids established from HLCs terminally differentiated at day 25 (d25orgs) compared to other organoids (d9orgs, d14orgs) (Fig. S4). The results of immunofluorescent staining and FACS analysis of albumin and CYP3A4 suggested that the majority of iHOs cultured with Hep-Medium were hepatocytes (Fig. S5). Thus, we concluded that iHOs established from terminally differentiated HLCs (day25) would be the most suitable for the generation of the hepatocytes with higher hepatic functions.

### 2.2. Two-dimensional culture of iHOs

Organoid culture embedded in Matrigel is difficult to apply to pharmaceutical research due to sequestration of the drugs in the gels, low throughput, and limited available evaluation systems. In contrast, 2D-cultured cells can be used for many existing applications, such as high throughput screening in multi-well plates.

In this section, to enable wider application of iHOs in pharmaceutical research, we attempted to culture iHOs under 2D condition. Hep-Medium-cultured iHOs were dissociated into single cells and seeded into multi-well plates. We first attempted 2D culture with Hep-Medium or Diff-Medium (Figure S6 A), but the 2D-cultured cells were largely stacked (Figure S6 B) and their hepatic gene expressions and CYP3A4 enzymatic activity were low (Figure S6 C, D). Therefore, we tried another method. We applied an 11-day culture protocol with stepwise addition of multiple growth factors and chemicals (Fig. 2A), which was recently established by our group using PHH-derived organoids [33]. After 2D culture with the Stepwise-Medium, the iHO-derived two-dimensionally cultured cells (iHO-Heps) showed a hepatocyte-like polygonal morphology similar to that of HLCs (Fig. 2B and Fig. S6B).

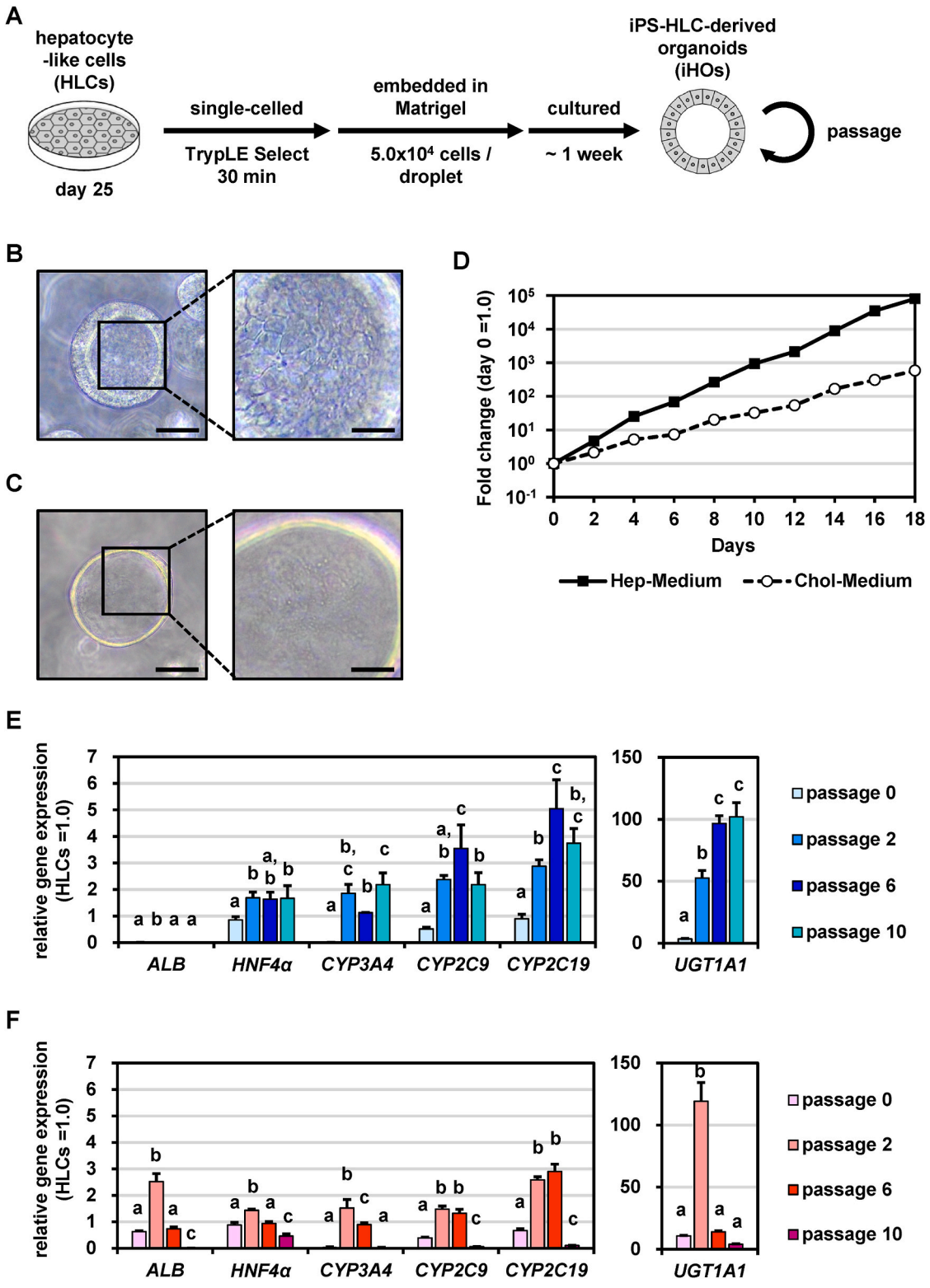


**Fig. 1.** Suitable media for the establishment and culture of hepatic organoids. (A) Schematic overview of the protocol for establishment of hepatic organoids, called iHOs, from human iPS cell-derived hepatocyte-like cells (HLCs). iHOs were established and cultured with Hep-Medium or Chol-Medium. (B, C) Phase-contrast micrographs of iHOs established and maintained by Hep-Medium (B) or Chol-Medium (C). The left panel is at lower magnification (50 μm) and the right panel at higher magnification (scale bar = 20 μm). (D) Growth curve of iHOs from day 0 to day 18 after passage. (E, F) The gene expression levels of hepatocyte (*ALB*, *HNF4α*, *CYP3A4*, *CYP2C9*, *CYP2C19*, *UGT1A1*) markers were examined in iHOs cultured for several passages (0, 2, 6, and 10 passages) with Hep-Medium (E) or Chol-Medium (F) by real-time RT-PCR. The gene expression levels in HLCs were taken as 1.0. Data represent the means ± SD (n = 3, biological replicates). Statistical significance was evaluated by one-way ANOVA followed by Tukey's post-hoc tests to compare all groups. Groups that do not share the same letter are significantly different from each other ($p < 0.05$).

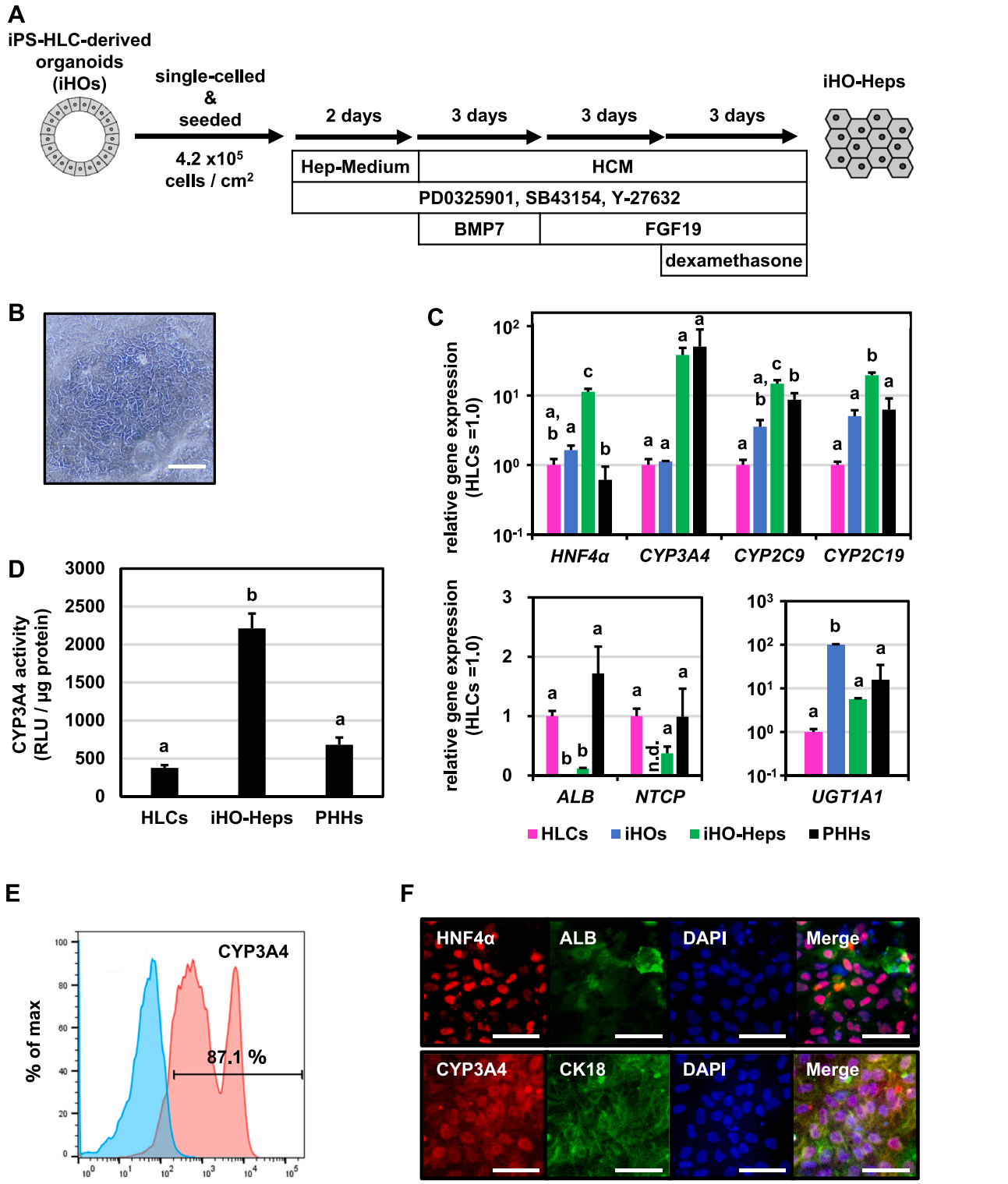


**Fig. 2.** Two-dimensional culture of iHOs. (A) Schematic overview of the protocol for 2D culture of iHOs. (B) Phase-contrast micrographs of the iHOs-derived 2D-cultured cells (iHO-Heps). Scale bar = 50 μm. (C) The gene expression levels of hepatocyte (*ALB*, *HNF4α*, *CYP3A4*, *CYP2C9*, *CYP2C19*, *NTCP*, *UGT1A1*) markers were examined in HLCs, iHOs cultured with Hep-Medium, iHO-Heps, and PHHs by real-time RT-PCR. The data of PHHs was an average of the three lots. The gene expression levels in HLCs were taken as 1.0. (D) CYP3A4 activity in HLCs, iHO-Heps, and PHHs. The data of PHHs was an average of the three lots. (E) Percentage of CYP3A4-positive cells in iHO-Heps by FACS analysis. (F) Expression of hepatocyte (ALB, HNF4α, CYP3A4, CK18) markers in iHO-Heps by immunohistochemistry. Scale bar = 50 μm. Data represent the means ± SD (n = 3, biological replicates). Statistical significance was evaluated by one-way ANOVA followed by Tukey's post-hoc tests to compare all groups. Groups that do not share the same letter are significantly different from each other ($p < 0\ 0.05$).

iHO-Heps cultured with Stepwise-Medium showed significantly higher hepatic gene expressions and CYP3A4 activity than iHO-Heps cultured in Hep-Medium or Diff-Medium (Figs. S6C and D). In the following experiments, we used Stepwise-Medium for iHO-Heps.

The gene expression levels of HNF4α and CYP enzymes in iHO-Heps were comparable or higher than those in HLCs, iHOs and even PHHs (Fig. 2C). Importantly, this trend was observed in iHO-Heps generated from organoids with different numbers of passages (5–15 passages) (Fig. S7B), suggesting that highly functional 2D-hepatocytes could be generated even when the iHOs were passaged 15 times. Interestingly, some hepatic gene expression levels in iHOs varied depending on the passage number of organoids (Fig. S7A). However, when these iHOs were 2D-cultured, the hepatic gene expression levels increased to similar levels regardless of passage number (Fig. S7B), suggesting that even if the hepatic gene expression in the iHOs differed from passage to passage, it was homogenized to a high level by 2D culture with Stepwise-Medium. In addition, the gene expression of sodium taurocholate co-transporting polypeptide (NTCP) was undetectable in iHOs but recovered to levels comparable to PHHs in iHO-Heps. The ALB gene expression, which was decreased in the iHOs, was restored by 2D culture, although it was still lower than that in the HLCs (Fig. 2C). Similar to the gene expression trend, the activity of CYP3A4, an enzyme important for drug metabolism, was significantly higher in iHO-Heps than in HLCs or PHHs (Fig. 2D), suggesting that iHO-Heps are suitable for application to drug discovery research. FACS analysis confirmed that nearly 90 % of cells in iHO-Heps were positive for CYP3A4 protein expression (Fig. 2E). The immunofluorescence staining confirmed the expression of hepatocyte marker proteins (ALB, HNF4α CYP3A4, and CK18) in iHO-Heps (Fig. 2F). Furthermore, the cryopreserved iHOs proliferated even after thawing and could be cultured under the 2D condition. Hepatic gene expression levels in cryopreserved iHOs after 2D culture remained high. The gene expression levels of CYP3A4, CYP2C9, and CYP2C19 and the level of CYP3A4 activity in cryopreserved iHOs after 2D culture were similar to those in PHHs (Figs. S8B and C).

On the other hand, when Chol-Medium-cultured-iHOs were cultured in 2D, they had lower hepatocyte marker gene expressions and CYP3A4 activity than HLCs (Fig. S9), suggesting that the medium used to maintain the organoids is important for generating iHO-Heps with higher hepatic functions. Establishment of iHOs using Hep-Medium and functional enhancement by 2D culture with an optimized protocol were confirmed in HLCs derived from another iPS cell line YOW-iPS (Fig. S10), suggesting the robustness of the protocol in this study.

### 2.3. Hepatic functions of iHO-Heps

We assessed various major hepatic functions in iHO-Heps. The majority of iHO-Heps stained positive with periodic acid-Schiff (PAS), confirming their glycogen storage capacity (Fig. 3A). The indocyanine green (ICG) test demonstrated that iHO-Heps had the capacity to uptake and release ICG (Fig. 3B). The albumin secretion level in iHO-Heps was sufficient for detection, although not as high as in HLCs and PHHs (Fig. 3C). The urea secretion level in iHO-Heps was also not comparable to that in PHHs but was higher than in HLCs (Fig. 3D). Formation of bile canaliculus in iHO-Heps was also confirmed by the measurement of bile acid excretion using 5(6)-carboxy-2′,7′-dichlorofluorescein diacetate (CDFDA), when iHOs were cultured in 2D for 11 days, followed by sandwich culture for 9 days. Inhibition of the function of MRP2, one of the bile acid excretion transporters, by MK-571 prevented the accumulation of CDFDA in the bile canaliculus (Fig. S11). These results suggested that iHO-Heps were mature hepatocytes with major hepatic functions.

We investigated the differences in hepatic functions after 2D culture among organoids established from cells at different hepatic differentiation stages (day9, day14, day25). The CYP3A4 activity, albumin secretion, and urea secretion all tended to be highest in organoids established from day 25 differentiated cells (d25org-Heps) (Fig. S12). In particular, albumin secretion in d25org-Heps was significantly higher than that in d9org-Heps and d14orgs-Heps (Fig. S12C). Again, it was confirmed that iHOs established from terminally differentiated HLCs (day25) would be the most suitable for the generation of highly

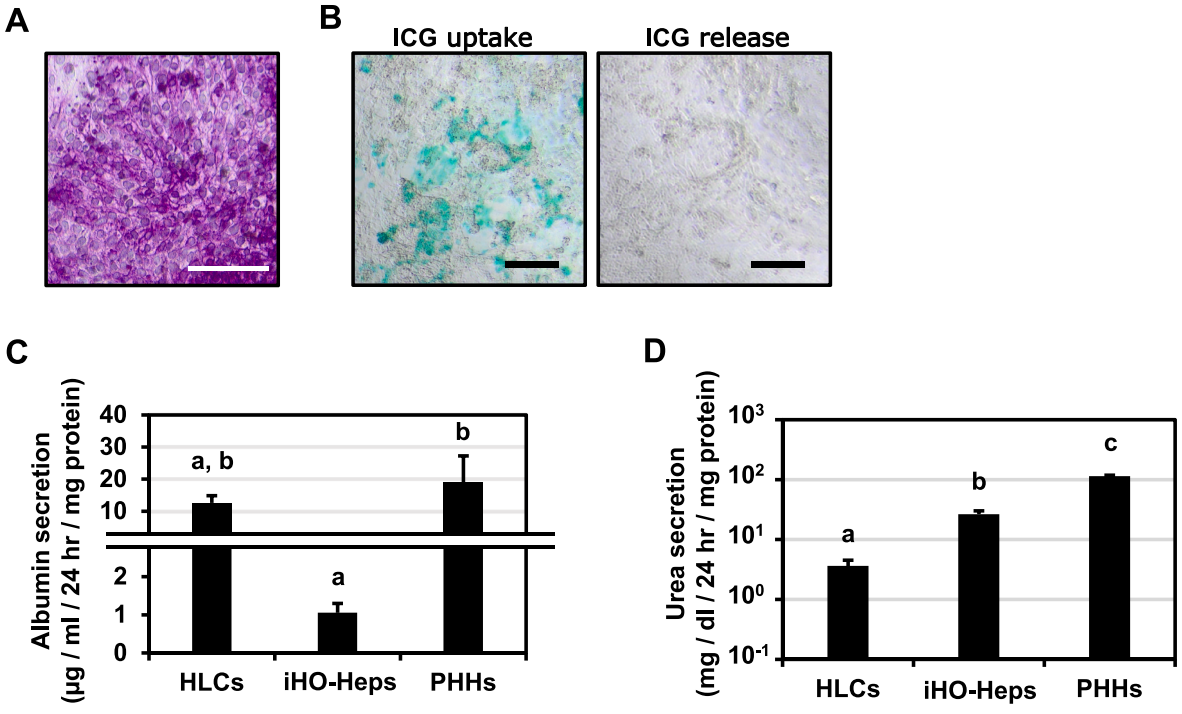


**Fig. 3.** Hepatic functions of iHO-Heps. (A) Cytoplasmic accumulation of glycogen in iHO-Heps was determined by PAS staining. Scale bar = 50 μm. (B) The capacity for the uptake (left) and release (right) of ICG was examined in iHO-Heps. Scale bar = 200 μm. (C, D) The amount of albumin (C) or urea (D) secretion was examined in HLCs, iHO-Heps, and PHHs. Data represent the means ± SD (n = 3, biological replicates). Statistical significance was evaluated by one-way ANOVA followed by Tukey's post-hoc tests to compare all groups. Groups that do not share the same letter are significantly different from each other ($p < 0.05$).

functional iHO-Heps.

### 2.4. Drug metabolism capacity and drug responsiveness of iHO-Heps

To evaluate the enzymatic activities of multiple CYPs in iHO-Heps, we used a cocktail of CYP model substrates (midazolam, diclofenac sodium salt, S-mephenytoin, and resorufin ethyl ether) and measured their representative metabolites (1-hydroxy midazolam, 4-hydroxydiclofenac, 4-hydroxymephenytoin, resorufin sodium salt) by liquid chromatography tandem mass spectrometry (LC-MS/MS). The results showed that the CYP enzymatic activities were greatly increased in iHO-Heps compared to HLCs. The levels of CYP3A4 and CYP2C19 enzymatic activities in iHO-Heps were especially elevated compared to those in PHHs (Fig. 4A).

Next, the hepatotoxic drug responsiveness in iHO-Heps was compared with that in PHHs. iHO-Heps and PHHs were exposed to four hepatotoxic drugs (acetaminophen, amiodarone, troglitazone, and desipramine). The susceptibility of iHO-Heps to acetaminophen was lower than that of PHHs under low concentration conditions, but the difference tended to be smaller under high concentration conditions (Fig. 4B). The susceptibility of iHO-Heps to amiodarone and troglitazone was comparable or higher than that of PHHs (Fig. 4B). At all desipramine concentrations, the cell viability of iHO-Heps was higher than that of PHHs (Fig. 4B). Note that, since desipramine is itself hepatotoxic and is detoxified by CYP2D6 [34], iHO-Heps would have higher sensitivity to desipramine than PHHs. This result was supported by higher level of CYP2D6 gene expression in iHO-Heps as compared with that in PHH, although the differences were not significant (Fig. S13).

We also examined the effects of long-term culture of iHO-Heps on cell morphology and CYP3A4 activity. iHO-Heps had a hepatocyte-like polygonal morphology until day 20 of 2D culture (Fig. 4C). The CYP3A4 activity in iHO-Heps at day 11 and day 20 of 2D culture was significantly higher than that in HLCs and PHHs (Fig. 4D). These results suggested that the iHO-Heps had a higher or similar capacity to metabolize drugs than HLCs or PHHs, respectively, and that iHO-Heps and PHHs responded to a similar range of hepatotoxic drugs, suggesting that iHO-Heps are suitable for studying the metabolism and response of a variety of drugs.

### 2.5. RNA-seq analysis of HLCs, iHOs, and iHO-Heps

To comprehensively profile the variation in gene expression by establishing organoids from HLCs and by 2D culture of organoids, we performed RNA-seq analysis on HLCs, iHOs, and iHO-Heps. Sequence data were divided into eight clusters by k-means clustering (Fig. 5A), and KEGG pathway analysis was performed for representative clusters (Fig. 5B). The results showed that pathways involved in metabolism by CYP enzymes such as “Metabolism of xenobiotics by cytochrome P450” and “Drug metabolism – cytochrome P450” were significantly enriched in cluster 1, indicating that these pathways are activated in iHO-Heps. For activation of metabolic pathways other than drug metabolism, cluster 2 included the “Mineral absorption” pathway, and cluster 3 included the “Metabolic pathways”, “Biosynthesis of amino acids”, “Biosynthesis of cofactors”, “Glycine, serine and threonine metabolism”, “Aminoacyl-tRNA biosynthesis”. Cluster 4 showed a significant enrichment of pathways involved in cell proliferation such as “Cell cycle”, “DNA replication” and “P53 signaling pathway”, indicating that these pathways were activated in iHOs. Cluster 6 showed significant enrichment of pathways involved in cell-to-cell and cell-to-matrix binding such as “Focal adhesion” and “Gap junction”, suggesting that HLCs formed a more robust cell structure than the other groups. Cluster 8 showed significant enrichment of various pathways such as “Complement and coagulation cascades”, “Apelin signaling pathway”, “AGE-RAGE signaling pathway in diabetic complications”, “ECM-receptor interaction” and “Cholesterol metabolism”.

Then, we analyzed differentially expressed genes (DEGs) between the two groups. The results showed that the DEGs between iHOs and HLCs (iHOs vs HLCs) contained 1545 down-regulated genes and 1353 up-regulated genes (Fig. 5C). The DEGs between iHO-Heps and iHOs (iHO-Heps vs iHOs) contained 1679 down-regulated genes and 1780 up-regulated genes (Fig. 5D). KEGG pathway analysis of these DEGs showed that pathways involved in protein synthesis such as “Ribosome” and “Aminoacyl-tRNA biosynthesis” are activated by the establishment of organoids from HLCs (Fig. 5E). These pathways were suggested to be activated in response to high cell proliferation in iHOs. Furthermore, 2D culture of organoids suppressed proliferation-related pathways and activated metabolic pathways including CYP enzymes (Fig. 5F). Thus, it was considered that 2D culture of organoids switched the cell state from a proliferative state to a metabolic state. A detailed comparison of the expression levels of metabolic and transport-related genes mainly act in hepatocytes was included in Fig. S14.

## 3. Discussion

In this study, we used organoid technology to overcome the challenges of HLCs and established an optimal culture protocol for iHOs that allowed cell proliferation and high hepatic gene expression. In addtion, we developed a 2D culture protocol with Stepwise-Medium for maturing iHOs into functional hepatocytes and demonstrated the utility of iHOs for pharmaceutical researches, such as drug metabolism and toxicity tests. In the past, pharmaceutical research using HLCs required differentiation of HLCs from iPS cells for each experiment. iHOs also require HLCs for establishment, but once iHOs are established, they can be expanded and maintained for approximately 3 months, and highly functional hepatocytes can be generated from these organoids in an 11-day 2D culture, as shown in the present study.

We examined the timing of organoid establishment and maintenance medium, and succeeded in generating iHOs that have both high cell proliferation capacity and high hepatic gene expression. Most previous reports used endodermal cells in the early stage of hepatic differentiation to establish human iPS cell-derived hepatic organoids [19,21,22,24]. The present study demonstrated that cells in a later stage of differentiation are more suitable as the source for establishing organoids which have higher hepatic functions, such as high expression levels of drug-metabolizing enzymes (Fig. S4).

The hepatic organoids generated in this study matured into functional hepatocytes by 2D culture with the optimized protocol, and the hepatocytes possessed most of the major hepatic functions, including albumin secretion, urea secretion, bile canaliculi formation, glycogen storage, and transporter activity, as well as drug metabolizing enzyme activities comparable to or higher than those of PHHs. Importantly, maturation of iHOs by 2D culture was only possible in optimized Stepwise-Medium and could not be reproduced in organoid culture media such as Hep-Medium or Diff-Medium (Fig. S6). The effect of Stepwise-Medium on iHOs was also examined, and we found that hepatic genes were upregulated even under organoid culture conditions as well as under 2D culture conditions (Fig. S15). This suggests that the culture medium is important to improve the functions of iHOs and that culture conditions—namely, the use of 2D vs 3D culture conditions—are largely irrelevant. Some of the in vitro assays can be performed in 3D organoids matured by the Stepwise-Medium. Nevertheless, compared to organoids, 2D cultured cells can be used for a wider variety of applications, especially for the pharmaceutical applications, such as ADME/Tox studies. We believe that the 2D culture protocol developed in this study has increased the versatility of iHOs.

In this study, the establishment of organoids from HLCs reduced the expression of albumin to less than 1/1000th of its original level (Fig. 1E). Although albumin expression in these organoids increased more than 100-fold when cultured in two dimensions, it did not reach a level comparable to that in HLCs (Fig. 3C). There are several possible reasons for the decreased expression of albumin by organoid establishment. The first is that the expression of cholangiocytes/progenitor

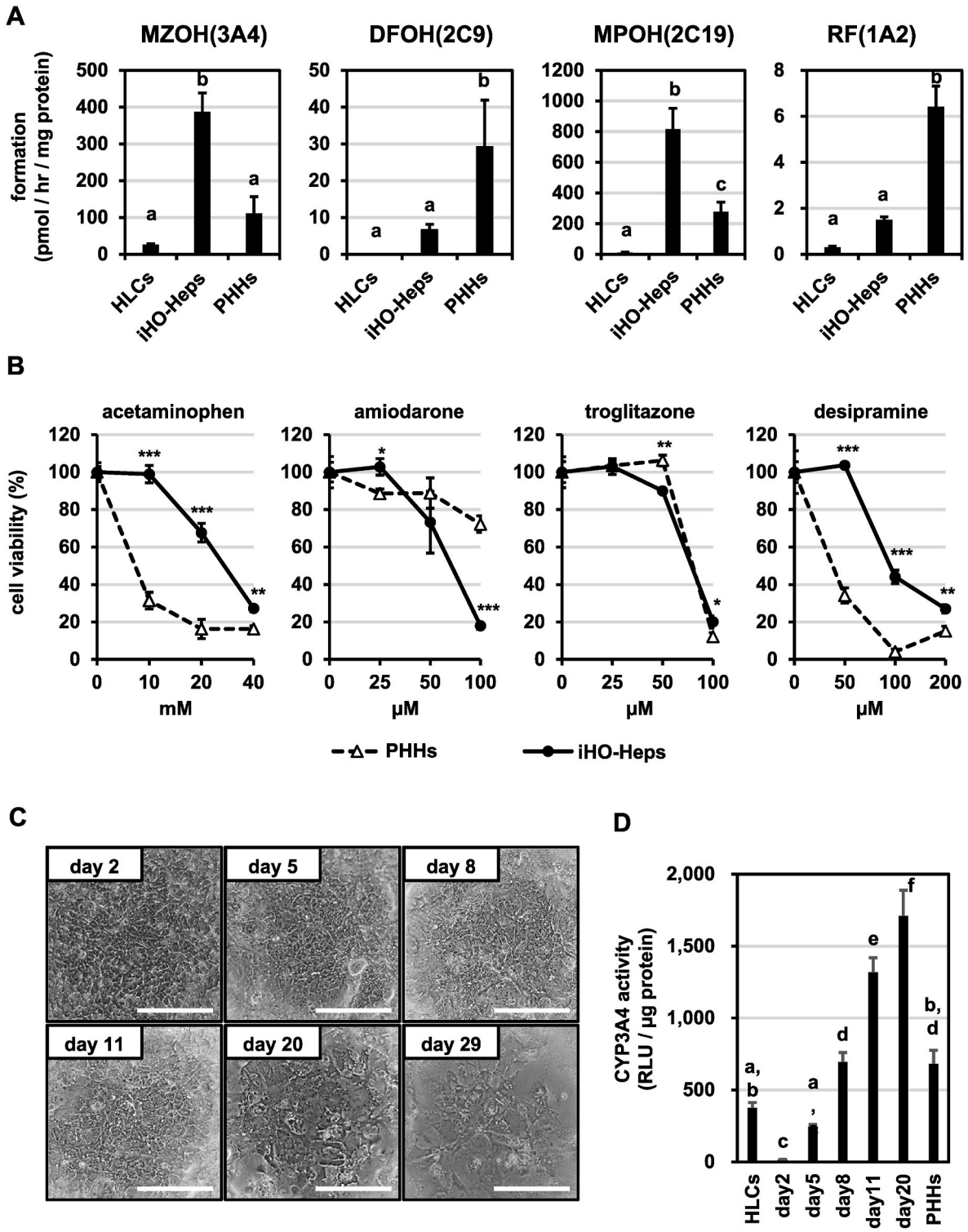


**Fig. 4.** Drug metabolism capacity and drug responsiveness of iHO-Heps. (A) The CYP3A4, CYP2C9, CYP2C19 and CYP1A2 activity levels in HLCs, iHO-Heps and PHHs were measured using each specific substrate by LC-MS/MS analysis. (B) The cell viability of iHO-Heps and PHHs was assessed by WST-8 assay after 24 h of exposure to different concentrations of acetaminophen, amiodarone, desipremine and troglitazone. Cell viability is expressed as a percentage of cells treated with solvent alone. (C) Phase-contrast micrographs of iHO-Heps at day 2, 5, 8, 11, 20, and 29 after seeding. Scale bar = 200 μm. (D) The CYP3A4 activity was examined in HLCs, iHO-Heps (at days 2, 5, 8, 11, and 20 after seeding), and PHHs. The CYP3A4 activity of PHHs was an average of the three lots. Other data of PHHs were from lot HUM183221. Data represent the means ± SD (n = 3, biological replicates). Statistical significance was evaluated by unpaired two-tail Student's t-test (*$p < 0.05$, **$p < 0.01$, ***$p < 0.005$: compared with "PHHs") or unpaired one-way ANOVA followed by Tukey's post-hoc tests to compare all groups. Groups that do not share the same letter are significantly different from each other ($p < 0.05$).

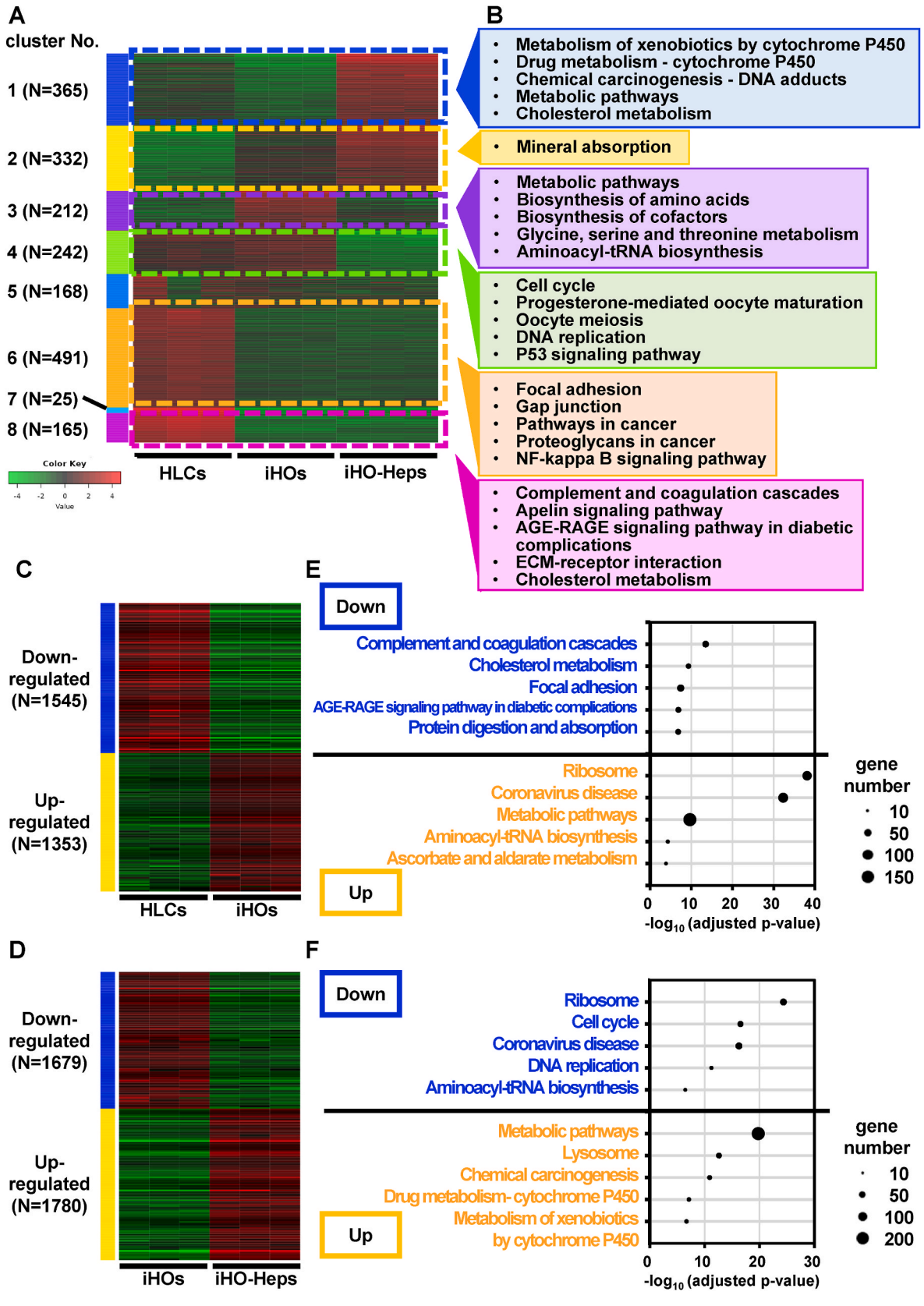


(caption on next page)

**Fig. 5.** RNA-seq analysis of HLCs, iHOs, and iHO-Heps. (A) The top 2000 most variable genes across all samples were visualized by heatmap and k-means clustering. Gene expression variation was calculated by Z-score, with red indicating an increase in expression compared to the mean across all samples, and green indicating a decrease in expression. (B) KEGG pathway analysis of enriched clusters 1, 2, 3, 4, 6, and 8. The top 5 KEGG pathways are shown in order of decreasing adjusted P-value. Cluster 2 contained only one pathway. The adjusted P-value was <0.005 for all pathways. (C) A heatmap illustrating differentially expressed genes (DEGs) between the iHOs and HLCs groups. Blue represents the down-regulated DEGs and yellow represents the up-regulated DEGs. (D) Heatmap illustrating differentially expressed genes (DEGs) between the iHO-Heps and iHOs groups. Blue represents the down-regulated DEGs and yellow represents the up-regulated DEGs. (E) Enriched bubble chart of the top 5 KEGG pathways of down- or up-regulated DEGs between the iHOs and HLCs groups. The y-axis is the enriched pathway, and the x-axis is the -log 10-adjusted P-value. The bubble size represents the gen number. (F) Enriched bubble chart of the top 5 KEGG pathways of down- or up-regulated DEGs between the iHO-Heps and iHOs groups. The y-axis is the enriched pathway, and the x-axis is the -log 10 adjusted P-value. The bubble size represents the gene number.

(*EpCAM, CK7, CK19, LGR5*) markers was increased in organoids in this establishment protocol (Fig. S2). This might have attenuated albumin expression. Second, the organoids established in this study had too-high cell proliferative potential (Fig. 1D), which could have suppressed cell maturation and led to the weakening of albumin expression.

iHO-Heps displayed a variety of hepatic functions, but some of these functions, such as albumin expression, were limited. FACS analysis showed that CYP3A4 expression levels in iHO-Heps were divided into two peaks. This suggests that iHO-Heps were not fully matured and that less differentiated hepatocytes were still present. In the future, therefore, it will be necessary to investigate the details of the mechanism of iHO-Heps maturation by Stepwise-Medium and further optimize the protocol.

Although several studies have been performed on human iPS cell-derived hepatic organoids [19,21–24], few have analyzed their drug-metabolizing capacity in detail. Kim et al. reported human iPS cell-derived hepatocyte organoids with drug-metabolizing enzyme activity comparable to that of PHHs [20], but the assay was performed in 3D culture, which was inefficient and had throughput too low for pharmaceutical research. The organoids generated in this study matured into functional hepatocytes in 2D culture with the optimized Stepwise-Medium and could be applied to various assays, including high-throughput screening, using the same conventional protocols as PHHs. Moreover, the organoids were expected to lead to robust drug discovery research because they showed stable functionality in 2D culture even after passage or cryopreservation. By applying a 2D organoid culture protocol that was recently developed by our group using PHH- or human liver biopsy-derived organoids [33], we have successfully developed iHO-Heps. iHO-Heps showed much higher expression and activity of drug-metabolizing enzymes than HLCs and iHOs, which was supported by the results of RNA-seq analysis.

In the present study, most functions in iHO-Heps were compared with those in PHHs at 48 h after seeding. This is because, in general, most pharmaceutical companies use PHHs cultured for 48–72 h for toxicity studies, while for metabolic studies they tend to use PHHs cultured for 0–6 h. The hepatic functions in 48 h-cultured PHHs are worse than those in 0 h-cultured PHHs. However, it can be argued that iHO-Heps is approaching a level of liver function that can be used for the ADME/Tox assay.

RNA-seq analysis confirmed that the establishment of organoids from HLCs activates cell proliferative capacity and that drug metabolism-related genes are highly expressed by 2D culture of organoids. In particular, it is very interesting that 2D-cultured organoids show improved hepatic functions compared to the original HLCs. We analyzed the genes that were specifically upregulated by the 2D culture of the organoids. We found 2021 up-regulated DEGs in iHO-Heps compared to HLCs and 1780 up-regulated DEGs compared to iHOs. Comparing the top 50 genes identified based on an ascending ranking of the P-values between the two sets of DEGs, we identified several common significantly upregulated genes (Fig. S16). Glutathione s-transferase A1 (GSTA1) is a phase II drug metabolizing enzyme specifically expressed in the liver and is a novel biomarker candidate for drug-induced liver injury (DILI) [35]. High expression of GSTA1 suppresses cell proliferation in hepatocyte carcinoma in vitro [36], and may be involved in the reduced cell proliferative capacity and enhanced drug-metabolizing capacity associated with 2D culture in iHOs. Less is known about the function of chromosome 1 open reading frame 115 (C1orf115) with the exception that this enzyme has been reported to modulate drug efflux through regulation of the major drug efflux factor multidrug resistance 1 (MDR1) [37], suggesting that it is indirectly involved in drug metabolism. Selenoprotein P (SELENOP) is the major plasma selenoprotein and is produced primarily in the liver, and coiled-coil domain containing 152 (CCDC152) is a translational regulator of SELENOP [38]. Since the liver is a central organ in selenium regulation and produces selenoproteins [39], the enhanced expression of these genes reinforces the maturation of iHO-Heps as hepatocytes. Other genes are not known to be associated with improved hepatic function in iHO-Heps, but some genes have been reported to be associated with hepatocellular carcinoma and cell proliferation [40–42]. These analyses of RNA-seq indicated that iHO-Heps acquire diverse hepatic functions compared to HLCs and iHOs.

In order to realize the wide application of human iPS cell-derived hepatocytes in pharmaceutical research, it is essential that cells with high hepatic function can be supplied in large quantities. Because iHOs have high cell proliferative capacity and mature into functional hepatocytes through 2D culture, they are expected to enable efficient and accurate prediction of the kinetics of drug candidate compounds. Furthermore, iHOs established from patient-derived or genome-edited iPS cells [31,43–46] will allow for the elucidation of the pathogenesis of inherited liver diseases and the prediction of idiosyncratic hepatotoxicity. Since iHOs can provide a large supply of highly functional hepatocytes, they might be suitable for hepatocyte transplantation in the future.

## 4. Materials and methods

### 4.1. Culture of human iPS cells

The human iPS cell lines Tic (obtained from the JCRB Cell Bank, JCRB Number: JCRB1331) and YOW-iPS [11] were maintained on 1 μg/cm$^2$ recombinant human laminin 511 E8 fragments (iMatrix-511, Nippi, Tokyo, Japan) with StemFit AK02 N medium (Ajinomoto). To passage human iPS cells, near-confluent human iPS cell colonies were treated with TrypLE Select Enzyme (Thermo Fisher Scientific) for 5 min at 37 °C. After centrifugation, human iPS cells were seeded at an appropriate cell density (5 × 10$^4$ cells/cm$^2$) onto iMatrix-511 and were then subcultured every 6 days.

### 4.2. Hepatic differentiation

The differentiation protocol for the induction of definitive endoderm cells, hepatoblast-like cells, and HLCs was based on our previous reports [11,28] with some modifications. Briefly, in the definitive endoderm differentiation, human iPS cells were cultured for 4 days with RPMI1640 medium (Sigma-Aldrich), which contained 100 ng/mL Activin A (R&D Systems), 2 × GlutaMAX (L-Alanyl-L-Glutamine, Thermo Fisher Scientific), and 0.5 × B27 Supplement Minus Vitamin A (Thermo Fisher Scientific). For the induction of hepatoblast-like cells, the definitive endoderm cells were cultured for 5 days with RPMI1640 medium containing 20 ng/mL BMP4 (R&D Systems), 20 ng/mL fibroblast growth

factor 4 (FGF4; R&D Systems), 2 × GlutaMAX (L-Alanyl-L-Glutamine), and 0.5 × B27 Supplement Minus Vitamin A. To perform hepatic differentiation, the hepatoblast-like cells were cultured for 5 days with RPMI1640 medium containing 20 ng/mL hepatocyte growth factor, 2 × GlutaMAX (L-Alanyl-L-Glutamine), and 0.5 × B27 Supplement Minus Vitamin A. Finally, the cells were cultured for 11 days with hepatocyte culture medium (HCM, Lonza) without EGF but with 20 ng/mL oncostatin M (OsM; R&D Systems) and 3 × GlutaMAX (L-Alanyl-L-Glutamine), generating HLCs.

### 4.3. Establishment of hepatic organoids from human iPS cell-derived HLCs

HLCs were dissociated into single cells using TrypLE Select Enzyme (Thermo Fisher Scientific) for 15 min and mechanical disruption with a pipette, and then passed through a 70 μm cell strainer (Falcon). After centrifugation at 500*g* for 5 min, the dissociated HLCs were mixed with Matrigel (Corning) and dispersed uniformly in the suspension by pipetting at least 20 times. The cells were then seeded in 24-well plates. The number of cells was $5.0 \times 10^4$ cells per 40 μL droplet per well. The cells were cultured with Hep-Medium or Chol-Medium. Diff-Medium was also used for maturation of the organoids cultured with Hep-Medium. These media were prepared based on previous reports [7, 32]. During cultivation, each medium was refreshed every 2–3 days. The organoids were passaged with a split ratio of 1:10 to 1:20 every 7 days. The composition of the media are listed in Table 1.

### 4.4. Passage of hepatic organoids

The organoids were passaged every 7 days. The organoid droplets were mechanically crushed by pipetting and dissociated using TrypLE Select Enzyme (Thermo Fisher Scientific) for 7 min. After dissociation, the organoids were pipetted again to uniformly disperse the cells into the suspension. After centrifugation at 500*g* for 5 min, the dissociated cells were mixed with Matrigel and dispersed uniformly in the suspension by pipetting at least 20 times. The cells were then seeded in 24-well plates at a split ratio of 1:10 to 1:20.

### 4.5. Cell-proliferation assessment

Organoids were passaged into 96-well plates with 10 μl droplets of organoids Matrigel mixture and 100 μl of medium per well. The medium was changed every two days. The CellTiter-Glo® 3D Cell Viability Assay (Promega) was used to assess organoid growth and viability every 2 days for 18 days according to the manufacturer's instructions. Luminescence was detected using a TriStar2 LB942 (Berthold Technologies).

### 4.6. Two dimensional culture of hepatic organoids

The hepatic organoids were dissociated into single cells using TrypLE Select Enzyme (Thermo Fisher Scientific) and mechanical disruption with a pipette, and then passed through a 70 μm cell strainer (Falcon). The 2D culture of hepatic organoids was performed according to our previous report using PHH-derived hepatic organoids [33]. Breifly, the cells were seeded at $4.2 \times 10^5$ cells/cm$^2$ in Matrigel-coated plates and cultured with Hep-Medium containing PD0325901 (0.5 μM, Wako), SB43154 (2 μM, Wako) and Y-27632 (10 μM, Wako) for 2 days. On day 2 after seeding, the cells were cultured with HCM (Lonza) without EGF but with 3 × GlutaMAX (L-Alanyl-L-Glutamine), PD0325901 (0.5 μM, Wako), SB43154 (2 μM, Wako), Y-27632 (10 μM, Wako) and BMP7 (50 ng/mL) for 3 days. Next, the cells were cultured with HCM (Lonza) without EGF but with 3 × GlutaMAX (L-Alanyl-L-Glutamine), PD0325901 (0.5 μM, Wako), SB43154 (2 μM, Wako), Y-27632 (10 μM, Wako) and FGF19 (100 ng/mL, PeproTech) for 3 days. Finally, the cells were cultured with HCM (Lonza) without EGF but with 3 × GlutaMAX (L-Alanyl-L-Glutamine), PD0325901 (0.5 μM, Wako), SB43154 (2 μM, Wako), Y-27632 (10 μM, Wako), FGF19 (100 ng/mL, PeproTech) and dexamethasone (10 μM, Wako) for 3 days.

### 4.7. Cryopreservation of hepatic organoids

The hepatic organoids were dissociated into single cells using TrypLE Select Enzyme (Thermo Fisher Scientific) and mechanical disruption with a pipette. The cells were suspended in 500 μL ($2.0 \times 10^5$ cells) of STEM-CELLBANKER (DMSO Free GMP grade, ZENOAQ) and transferred to a cryotube. The cryotube was placed into BICELL (Nihon Freezer Co., Ltd.) for slow freezing at −80 °C. After overnight incubation, the cryotube was transferred to a −150 °C freezer and cryopreserved more than 2 weeks. For thawing, the cryotubes were incubated at 37 °C for 1 min. The thawed cell suspension was transferred to 10 mL of PBS. After centrifugation, the cells were mixed with Matrigel (Corning) and seeded in 24 wells. The cell concentration was $5.0 \times 10^4$ cells/40 μL droplet.

### 4.8. Real-time RT-PCR

Total RNA was extracted from each cell population using ISOGENE (Nippon Gene). cDNA was synthesized from 500 ng of each total RNA by reverse transcription reaction using a Superscript VILO cDNA synthesis kit (Thermo Fisher Scientific). Target mRNA expression levels were quantified relatively using the 2-ΔΔCT method. Glyceraldehyde 3-phosphate dehydrogenase (GAPDH) was used as an internal standard gene. The primer sequences used for quantitative RT-PCR (Table 2) were obtained from PrimerBank (https://pga.mgh.harvard.edu/primerbank/).

### 4.9. Fluorescent assay for CYP3A4 activity

The CYP3A4 activity was measured using P450-Glo™ CYP3A4 Assay Kits (Promega). Luciferin-IPA was used as a substrate for CYP3A4, and fluorescence intensity was measured with a luminometer (Lumat LB 9507, Berthold). The CYP3A4 activity was calculated by normalizing to the protein content per well. Protein content was measured using Pierce BCA Protein Assay Kit according to the manufacturer's instructions.

### 4.10. Immunofluorescence

To perform the immunofluorescence, cells were washed twice with phosphate-buffered saline (PBS), treated with 4 % paraformaldehyde (PFA; FUJIFILM Wako Pure Chemical) for 10 min at room temperature. Cells were blocked with PBS containing 2 % BSA (Sigma-Aldrich) and 0.2 % Triton X-100 (Sigma-Aldrich) for 45 min. The cells were then reacted with primary antibody overnight at 4 °C, followed by secondary antibody (Thermo Fisher Scientific) labeling with Alexa Fluor 488 or Alexa Fluor 594 for 1 h at room temperature. Nuclear staining was then performed using 4′,6-diamidino-2-phenylindole (DAPI) (Thermo Fisher Scientific), and cells were observed under a fluorescence microscope (BIOREVO BZ-9000, Keyence). The antibodies used are listed in Table 3.

### 4.11. ALB secretion

The culture supernatants, which were incubated for 24 h after fresh medium was added, were collected and analyzed by enzyme-linked immunosorbent assay (ELISA) to determine their levels of ALB secretion. A Human Albumin ELISA Quantitation Set was purchased from Bethyl Laboratories. ELISA was performed according to the manufacturer's instructions. The amount of ALB secretion was calculated according to each standard followed by normalization to the protein content per well. Protein content was measured using a Pierce BCA Protein Assay Kit according to the manufacturer's instructions.

### 4.12. Urea secretion

The culture supernatants, which were incubated for 24 h after fresh

medium was added, were collected and analyzed to determine the amount of urea production. Urea measurement kits were purchased from BioAssay Systems. The measurement was performed according to the manufacturer's instructions. The amount of urea secretion was calculated according to each standard followed by normalization to the protein content per well. Protein content was measured using Pierce BCA Protein Assay Kit according to the manufacturer's instructions.

### 4.13. Periodic acid-Schiff staining

Cells were washed with PBS and stained using a Periodic Acid-Schiff (PAS) Staining System (Sigma-Aldrich) according to the instruction manual.

### 4.14. Cellular uptake and excretion of indocyanine green (ICG)

ICG (Sigma) was dissolved in DMSO at 100 mg/mL, then added to a culture medium of the iHO-Heps to a final concentration of 1 mg/mL. After incubation at 37 °C for 60 min, the medium with ICG was discarded and the cells were washed with PBS. The cellular uptake of ICG was then examined by microscopy. The phosphate-buffered saline was then replaced with culture medium and the cells were incubated at 37 °C for 16 h. The excretion of ICG was examined by microscopy.

### 4.15. Cell viability tests

The cell viability of the iHO-Heps was assessed by using WST-8 assay kit (Dojindo) after 24 h exposure to different concentrations of acetaminophen (Wako), amiodarone (Sigma), desipremine (Wako) and troglitazone (Wako). The control refers to incubations in the absence of test compounds and was considered as a 100 % viability value. Controls were treated with DMSO (final concentration 0.1 %).

### 4.16. FACS analysis

Single-cell suspensions of the cells were fixed with 2 % PFA at 4 °C for 10 min, and then incubated with the primary antibody, followed by the secondary antibody. Analysis was performed by using a FACS LSR Fortessa flow cytometer (BD Biosciences) and FlowJo software (FlowJo LLC, http://www.flowjo.com/). All the antibodies are listed in Table 3.

### 4.17. Measurement of the CYP enzymatic activities by LC-MS/MS analysis

The cells were treated with a cocktail of CYP model substrates (100 μM midazolam, 100 μM diclofenac sodium salt, 8 mM S-mephenytoin, and 50 μM resorufin ethyl ether) for 24 h and their representative metabolites (1-hydroxy midazolam, 4-hydroxydiclofenac, 4-hydroxymephenytoin, resorufin sodium salt) were measured by liquid chromatography tandem mass spectrometry (LC-MS/MS). LC-MS/MS data were obtained by mass spectrometry (Xevo TQ-S, Waters Corp., Milford, MA) connected to UPLC (ACQUITY UPLC, Waters), using a BEH C18 column (1.7 μm, 2.1 × 50 mm, Waters). Mobile phase A consisted of 0.1 % formic acid/water, and mobile phase B was 0.1 % formic acid/acetonitrile under the following gradient system: 0 min-2% B, 1.0 min-95 % B, 1.25 min-95 % B, 1.26 min-2% B, and 1.75 min-2% B. The flow rate was 1.0 mL/min.

### 4.18. RNA-sequencing analysis

According to the manufacturer's instructions, library preparation was performed using a TruSeq stranded mRNA sample prep kit (Illumina, San Diego, CA). Libraries were converted to libraries for DNBSEQ using an MGIEasy Universal Library Conversion Kit (App-A). Sequencing was performed on a DNBSEQ-G400RS platform (MGI, Shenzhen, China) in 2 x100 bp paired-end mode. RNA-Seq data were processed using Trimmomatic to trim low-quality bases and Illumina sequencing adapters from the 3′ end of the reads. Reads were mapped to GRCh38.p13 of the human genome using HISAT2 [47]. HISAT2 outputs were fed into featureCounts [48] for transcript quantification. DESeq2 [49] was used to product fragments per kilobase of exon model per million reads mapped (FPKM) values. The expression levels of each gene were calculated using the number of reads uniquely aligned with the reference gene. Uniquely mapped reads were quantified into counts for each gene, and transcripts per million (TPM) were used. iDEP.96[50](http://bioinformatics.sdstate.edu/idep96/) was used to create heatmaps and to conduct k-Means clustering and KEGG pathway enrichment analysis. In iDEP.96, DESeq2 was used to identify differentially expressed genes (DEGs). The Gene Expression Omnibus (GEO) accession number for the microarray analysis is GEO: GSE243384.

### 4.19. Primary human hepatocytes (PHHs)

Four lots of cryopreserved human hepatocytes (lots HC4-24; XENOTECH, lots HC10-10; XENOTECH, lots S1435T; Kaly-Cell, lots HUM183221; Lonza) were used. The former three lots were used for qRT-PCR assay and CYP3A4 activity assay. For the other experiments, HUM183221 (Lonza) was used. The vials of hepatocytes were rapidly thawed in a shaking water bath at 37 °C; the contents of each vial were emptied into prewarmed HCM and the suspension was centrifuged at 900 rpm for 10 min at room temperature. The hepatocytes were seeded at $1.25 \times 10^5$ cells/cm$^2$ in HCM containing 10 % FBS onto type I collagen (Nitta Gelatin)-coated 48-well plates. Human hepatocytes cultured for 48 h after plating were used in the experiments.

### 4.20. Statistical analysis

All results are based on three biological replicates. Statistical analysis was performed using the unpaired two-tailed Student's t-test or one-way ANOVA followed by Tukey's post-hoc tests. A value of $p < 0.05$ was considered statistically significant.

## CRediT authorship contribution statement

**Jumpei Inui:** Writing – review & editing, Writing – original draft, Visualization, Validation, Methodology, Investigation, Formal analysis, Data curation. **Yukiko Ueyama-Toba:** Writing – review & editing, Visualization, Validation, Methodology, Investigation, Funding acquisition, Formal analysis, Data curation, Conceptualization. **Chiharu Imamura:** Visualization, Investigation, Formal analysis. **Wakana Nagai:** Visualization, Investigation, Formal analysis. **Rei Asano:** Formal analysis, Investigation, Visualization. **Hiroyuki Mizuguchi:** Writing – review & editing, Writing – original draft, Supervision, Resources, Project administration, Funding acquisition, Conceptualization.

## Financial support statement

This research was financially supported by Japan Agency for Medical Research and development, AMED (grant number JP24fk0310512, JP24mk0121300); Platform Project for Supporting Drug Discovery and Life Science Research (Basis for Supporting Innovative Drug Discovery and Life Science Research (BINDS)) from AMED (grant number JP24ama121054); Japan Society for the Promotion of Science (JSPS) KAKENHI [grant number 21K18247]; Japan Science and Technology Agency SPRING [Grant Number JPMJSP2138].

## Declaration of competing interest

The authors declare that they have no known competing financial interests or personal relationships that could have appeared to influence the work reported in this paper.

## Acknowledgements

We thank Mr. Jumpei Yokota for his support in the RNA-sequencing analysis. We thank Ms. Yanran Tong for her support in the assay of bile canaliculi formation.

## Appendix A. Supplementary data

Supplementary data to this article can be found online at https://doi.org/10.1016/j.biomaterials.2025.123148.

## Data availability

Data will be made available on request.

## References

[2] R.J. Weaver, et al., Managing the challenge of drug-induced liver injury: a roadmap for the development and deployment of preclinical predictive models, Nat. Rev. Drug Discov. 19 (2019) 131–148.
[3] T. Katsuda, et al., Generation of human hepatic progenitor cells with regenerative and metabolic capacities from primary hepatocytes, Elife 8 (2019).
[4] C. Xiang, et al., Long-term functional maintenance of primary human hepatocytes in vitro, Science 364 (2019) 399–402.
[5] L. Broutier, et al., Culture and establishment of self-renewing human and mouse adult liver and pancreas 3D organoids and their genetic manipulation, Nat. Protoc. 11 (2016) 1724–1743.
[6] S. Rose, et al., Generation of proliferating human adult hepatocytes using optimized 3D culture conditions, Sci. Rep. 11 (2021) 515.
[7] H. Hu, et al., Long-term expansion of functional mouse and human hepatocytes as 3D organoids, Cell 175 (2018) 1591–1606.e19.
[8] W.L. Thompson, T. Takebe, Generation of multi-cellular human liver organoids from pluripotent stem cells, Methods Cell Biol. 159 (2020) 47–68.
[9] T. Tricot, C.M. Verfaillie, M. Kumar, Current status and challenges of human induced pluripotent stem cell-derived liver models in drug discovery, Cells 11 (2022) 442.
[10] J. Blaszkiewicz, S.A. Duncan, Advancements in disease modeling and drug discovery using iPSC-derived hepatocyte-like cells, Genes 13 (2022) 573.
[11] K. Takayama, et al., Prediction of interindividual differences in hepatic functions and drug sensitivity by using human iPS-derived hepatocytes, Proc. Natl. Acad. Sci. U.S.A. 111 (2014) 16772–16777.
[12] M. Baxter, et al., Phenotypic and functional analyses show stem cell-derived hepatocyte-like cells better mimic fetal rather than adult hepatocytes, J. Hepatol. 62 (2015) 581–589.
[13] D.R. Berger, B.R. Ware, M.D. Davidson, S.R. Allsup, S.R. Khetani, Enhancing the functional maturity of induced pluripotent stem cell-derived human hepatocytes by controlled presentation of cell-cell interactions in vitro, Hepatology 61 (2015) 1370–1381.
[14] M. Simian, M.J. Bissell, Organoids: a historical perspective of thinking in three dimensions, J. Cell Biol. 216 (2017) 31–40.
[15] A. Marsee, et al., Building consensus on definition and nomenclature of hepatic, pancreatic, and biliary organoids, Cell Stem Cell 28 (2021) 816–832.
[16] F. Wu, et al., Generation of hepatobiliary organoids from human induced pluripotent stem cells, J. Hepatol. 70 (2019) 1145–1158.
[17] X. Xu, et al., High-throughput bioengineering of homogenous and functional human-induced pluripotent stem cells-derived liver organoids via micropatterning technique, Front. Bioeng. Biotechnol. 10 (2022) 937595.
[18] T. Takebe, et al., Massive and reproducible production of liver buds entirely from human pluripotent stem cells, Cell Rep. 21 (2017) 2661–2670.
[19] R. Ouchi, et al., Modeling steatohepatitis in humans with pluripotent stem cell-derived organoids, Cell Metabol. 30 (2019) 374–384.e6.
[20] H. Kim, et al., Development of human pluripotent stem cell-derived hepatic organoids as an alternative model for drug safety assessment, Biomaterials 286 (2022) 121575.
[21] S. Akbari, et al., Robust, long-term culture of endoderm-derived hepatic organoids for disease modeling, Stem Cell Rep. 13 (2019) 627–641.
[22] S.J. Mun, et al., Generation of expandable human pluripotent stem cell-derived hepatocyte-like liver organoids, J. Hepatol. 71 (2019) 970–985.
[23] Y. Guan, et al., Human hepatic organoids for the analysis of human genetic diseases, JCI Insight 2 (2017).
[24] M. N. Bin Ramli, et al., Human pluripotent stem cell-derived organoids as models of liver disease, Gastroenterology 159 (2020) 1471–1486.e12.
[25] D. Abbey, S. Elwyn, N.J. Hand, K. Musunuru, D.J. Rader, Self-organizing human induced pluripotent stem cell hepatocyte 3D organoids inform the biology of the pleiotropic TRIB1 gene, Hepatol. Commun. 4 (2020) 1316.
[26] T. Takebe, et al., Vascularized and functional human liver from an iPSC-derived organ bud transplant, Nature 499 (2013) 481–484.
[27] T. Shinozawa, et al., High-fidelity drug-induced liver injury screen using human pluripotent stem cell–derived organoids, Gastroenterology 160 (2021) 831–846.e10.
[28] J. Inui, Y. Ueyama-Toba, S. Mitani, Hiroyuki Mizuguchi, Development of a method of passaging and freezing human iPS cell-derived hepatocytes to improve their functions, PLoS One 18 (2023) e0285783.
[29] T. Shintani, et al., Establishment of UGT1A1-knockout human iPS-derived hepatic organoids for UGT1A1-specific kinetics and toxicity evaluation, Mol. Ther. - Methods Clin. Dev. 30 (2023) 429–442.
[30] Y. Toba, et al., Comparison of commercially available media for hepatic differentiation and hepatocyte maintenance, PLoS One 15 (2020) e0229654.
[31] S. Deguchi, et al., In vitro model for a drug assessment of cytochrome P450 family 3 subfamily A member 4 substrates using human induced pluripotent stem cells and genome editing technology, Hepatol. Commun. 5 (2021) 1385–1399.
[32] M. Huch, et al., Long-term culture of genome-stable bipotent stem cells from adult human liver, Cell 160 (2015) 299–312.
[33] Y. Ueyama-Toba, et al., Development of a two-dimensional hepatic differentiation method from primary human hepatocyte-derived organoids for pharmaceutical research, iScience 27 (2024) 110778.
[34] E. Spina, et al., Relationship between plasma desipramine levels, CYP2D6 phenotype and clinical response to desipramine: a prospective study, Eur. J. Clin. Pharmacol. 51 (1997) 395–398.
[35] Y. Fu, F.-L. Chung, Oxidative stress and hepatocarcinogenesis, Hepatoma Res. 4 (2018) 39.
[36] X. Liu, et al., Glutathione S-transferase A1 suppresses tumor progression and indicates better prognosis of human primary hepatocellular carcinoma, J. Cancer 11 (2020) 83.
[37] S.N. Masud, et al., Chemical genomics with pyrvinium identifies C1orf115 as a regulator of drug efflux, Nat. Chem. Biol. 18 (2022) 1370–1379.
[38] Y. Mita, et al., Identification of a novel endogenous long non-coding RNA that inhibits selenoprotein P translation, Nucleic Acids Res. 49 (2021) 6893–6907.
[39] R.F. Burk, K.E. Hill, Regulation of Selenium Metabolism and Transport 35 (2015) 109–134, https://doi.org/10.1146/annurev-nutr-071714-034250.
[40] H. Wang, F. Xu, F. Yang, L. Lv, Y. Jiang, Prognostic significance and oncogene function of cathepsin A in hepatocellular carcinoma, Sci. Rep. 11 (2021) 1–15.
[41] Y. Zhang, et al., Sphingomyelin phodiesterase acid-like 3A promotes hepatocellular carcinoma growth through the enhancer of rudimentary homolog, Front. Oncol. 12 (2022) 852765.
[42] L.J. Wang, et al., Prognostic significance of sodium-potassium ATPaseregulator, FXYD3, in human hepatocellular carcinoma, Oncol. Lett. 15 (2018) 3024–3030.
[43] A. Ghodsizadeh, et al., Generation of liver disease-specific induced pluripotent stem cells along with efficient differentiation to functional hepatocyte-like cells, Stem Cell Rev. Reports 6 (2010) 622–632.
[44] R. Jing, et al., A screen using iPSC-derived hepatocytes reveals NAD+ as a potential treatment for mtDNA depletion syndrome, Cell Rep. 25 (2018) 1469–1484.e5.
[45] M.A. Cayo, et al., A drug screen using human iPSC-derived hepatocyte-like cells identifies cardiac glycosides as a potential treatment for hypercholesterolemia, Cell Stem Cell 20 (2017) 478.
[46] S. Deguchi, et al., Modeling of hepatic drug metabolism and responses in CYP2C19 poor metabolizer using genetically manipulated human iPS cells, Drug Metab. Dispos. 47 (2019) 632–638.
[47] D. Kim, J.M. Paggi, C. Park, C. Bennett, S.L. Salzberg, Graph-based genome alignment and genotyping with HISAT2 and HISAT-genotype, Nat. Biotechnol. 37 (2019) 907–915.
[48] Y. Liao, G.K. Smyth, W. Shi, featureCounts: an efficient general purpose program for assigning sequence reads to genomic features, Bioinformatics 30 (2014) 923–930.
[49] M.I. Love, W. Huber, S. Anders, Moderated estimation of fold change and dispersion for RNA-seq data with DESeq2, Genome Biol. 15 (2014) 1–21.
[50] S.X. Ge, E.W. Son, R. Yao, iDEP: an integrated web application for differential expression and pathway analysis of RNA-Seq data, BMC Bioinf. 19 (2018) 1–24.